Diffusion Motions and Microphase Separation of Styrene–Butadiene Diblock Copolymer in Solution. 2. Behavior in *n*-Decane in the Dilute Solution Region

Yoshisuke Tsunashima

Institute for Chemical Research, Kyoto University, Uji, Kyoto-fu 611, Japan

Received September 25, 1989; Revised Manuscript Received December 12, 1989

ABSTRACT: The dilute solution properties observed by dynamic light scattering spectroscopy at 25 °C are reported for a styrene–butadiene (SB) diblock copolymer (M_w = 9.73 × 10⁴, a styrene content of 29.3 wt %) in *n*-decane, a selective solvent to the B subchain. A double-step transition of the diffusion coefficient is assured as a function of the polymer concentration in the range from 1 × 10⁻⁶ to 7.24 × 10⁻³ g cm⁻³. The SB diblock copolymer is able to disperse molecularly only at an extremely dilute concentration of c < 3.8 × 10⁻⁶ g cm⁻³, while at a relatively dilute concentration of c > 1.1 × 10⁻⁴ g cm⁻³ the copolymer forms near-monodisperse micelles. The micelles are an intermolecular association of 100 pieces of SB copolymers and are constructed from a hard core of S subchains surrounded by swollen B subchains. The micellar size analyzed with a "two-phase" concentric sphere model indicates that the core radius is 10.2 nm, the shell thickness is 33.3 nm, and the apparent radius of gyration of the micelle as a whole is 33.8 nm; the B subchains are in a highly extended state in the shell. Moreover, the micelle shows internal motions which might be mainly due to the relative center-of-mass motion of the B subchains with respect to the S subchains in the micellar particle, i.e., due especially to the concentration fluctuation taking place in the shell. The concentration fluctuation may be caused by high chain flexibility of B subchains which swell highly in the shell.

I. Introduction

In dilute solutions of selective solvents, diblock copolymers form micelles (the intermolecular association) due to the different solubility of the component subchains to the solvents,[1–6] and the micellar formations have been investigated mainly[1–5] by light scattering, viscometry, sedimentation, and small-angle X-ray scattering and partly[6] by dynamic light scattering. Generally, the micelles in dilute solutions are considered to be of spherical shape and are rather compact. On the other hand, there should be a particle state where the diblock copolymers disperse in solution molecularly. Since a critical micellar concentration (cmc) has been detected experimentally in the micellization of both soaps and ionic and nonionic surfactants,[7] the single copolymer molecule would be expected to be in such a closed association type of micellization[8] as is characterized by an equilibrium between a molecularly dispersed copolymer and associations of N pieces of copolymers. It was examined theoretically for the diblock copolymers[9,10] that the molecular dispersion and the pronounced *microphase segregation* in the single molecule can take place only in *selective* solvents in a *very dilute* solution. Experimentally, however, there is little evidence that the diblock copolymer disperses molecularly in selective solvents. The reason is that, in most cases, the concentration dependences of measured values did not exhibit any major anomalies within the dilute concentration region studied, and the characteristic values were obtained by the simple extrapolation of the data to "infinite dilution". An exception is the results reported by Plestil and Baldrian[4] through sedimentation velocity measurements for a styrene–butadiene (SB) diblock copolymer (M_n = 6.5 × 10⁴) in *n*-heptane (selective to PB), where two types of particles *coexist* in the concentration range 5.4 × 10⁻³–3.83 × 10⁻² g cm⁻³: micelles and single molecule. It is interesting to note here that the two types of particles were also observed through sedimentation velocity measurements for SBS triblock copolymers in methyl ethyl ketone (selective to PS)[11] and in mixed solvents, dioxane/ethanol (selective to PS)[12] or THF/allyl alcohol (selective to PS).[13]

In a previous paper,[14a] the dynamical properties (translational diffusions and intrinsic viscosity) of a SB diblock copolymer (M_w = 9.73 × 10⁴) in *n*-decane (selective solvent of PB) were observed at 25 °C in the extremely dilute polymer concentration ranging from 1 × 10⁻⁶ to 5.7 × 10⁻⁴ g cm⁻³. The first cumulants (the decay rates of the autocorrelation functions) in dynamic light scattering $\Gamma(q,c)$, which were measured as functions of the scattering vector q ($q = (4\pi n_0/\lambda_0) \sin(\theta/2)$) and the polymer mass concentration c, exhibited anomalies in their concentration dependences. The $\Gamma(q,c)$ vs c curves became discontinuous twice around c_1 = 3.8 × 10⁻⁶ and c_2 = 1.1 × 10⁻⁴ g cm⁻³, and the extrapolations of $\Gamma(q,c)$ to "infinite dilution" did not give the sole way but ramified into a few branches, depending on the concentration regions to be treated. The diffusion coefficients determined by $\Gamma(q,c)$ values at q = 0 showed a double-step transition as a function of c, accordingly. In extremely dilute solutions of c < 3.8 × 10⁻⁶ g cm⁻³ (region I), the SB diblock copolymer was found to disperse molecularly, while in relative dilute solutions of c > 1.1 × 10⁻⁴ g cm⁻³ (region III) there was strong indication that the copolymer forms micelles. Coexistence of these two types of particles was never detected within the concentration region examined.

In this paper, the previously studied diblock copolymer/selective solvent system[14a] SB/*n*-decane is used. By dynamic light scattering, the hydrodynamical behavior of this system is investigated in a usual dilute solution region, i.e., in a higher polymer concentration region than that examined previously (extending from 2.1 × 10⁻⁴ to 7.24 × 10⁻³ g cm⁻³ and constituting the previously mentioned concentration region III). The purpose of the present study is thus to examine in more detail the q and c dependences of $\Gamma(q,c)$ and to complete the double-step transition behavior of the diffusion coefficient $D(c)$ ($=\Gamma(q=0,c)/q^2$) as a function of c in the wide range c = 1 × 10⁻⁶–7.24 × 10⁻³ g cm⁻³.[15] The simple extrapolation

0024-9297/90/2223-2963$02.50/0

of $D(c)$ to $c = 0$ within the concentration region III signifies the translational diffusion coefficient of the micelles as a whole. The micellar size deduced from the $D(c=0)$ value gives information about the microstructure of micelles, which structure is discussed in some detail with a "two-phase" spherical model. On the other hand, the behavior of $\Gamma(q,c)$ at larger q and c implies existence of new intramolecular motions in the micellar particle. The motions might come mainly from the relative center-of-mass motion of the outer part (the shell) of swollen B subchains with respect to the inner compact core of collapsed S subchains, which is also inspected.

II. Experimental Section

Materials. A monodisperse diblock copolymer sample of styrene (S) and butadiene (B), coded as SB1, was used for the present studies. The sample has been characterized previously in detail;[14a] its weight-average molecular weight M_w and the styrene content were 9.73×10^4 and 29.3 wt %, respectively. A solvent used was n-decane, which is good and selective for B subchains but is a precipitant for S subchains. Its purity was also checked previously:[14a] the refractive index n_0 (488 nm) = 1.4111, the density $d = 0.726\,25$ g cm^{-3}, and the viscosity $\eta_0 = 0.8543 \times 10^{-2}$ g cm^{-1} s^{-1} at 25 °C.

Preparation of Sample Solutions. An original solution was first prepared as follows: Weighed amounts of freeze-dried SB1 and n-decane were sealed in a dust-free test tube under N_2 atmosphere and then heated at ca. 50 °C for a few days until a homogeneous solution opalescent to clear light appeared, after which treatment the solution retained its scattering intensity unchanged. Next, sample solutions of different polymer concentration were made through dilution of the original solution in a nitrogen-filled drybox: the desired amount of the original solution was filtered into dust-free dynamic light scattering cells through a Millipore filter of 0.45-μm pore size and was mixed with the desired amount of n-decane which was put in advance into the cells through a 0.22-μm Millipore filter. Finally, the mixed solutions were heated again overnight at ca. 50 °C. Here the dust-free cells were prepared with a modified Thurmond glass still,[34] in which still filtered methanol was refluxed continuously and the cells were rinsed repeatedly by the flushly distilled methanol.

Methods. The normalized autocorrelation functions $A(\tau)$ of the scattered light (V_v component) from the solutions were measured at 25 °C on our laboratory-made 512-channel time-interval correlator with a 488-nm single line emitted from an etalon-equipped argon ion laser.[14b] The correlator counts with a time interval digitizer the time intervals between neighboring pulses in an input pulse train of the scattered light.[14b] The scattering angles measured were six fixed angles of 10°, 30°, 60°, 90°, 120°, and 150°. The sample cells were selected precision-cylinder NMR tubes of 12-mmϕ outer diameter (inner diameter = 11 mmϕ). Optical alignment at $\theta = 10°$ with the cells gave an error of ±2.5% in the evaluation of the decay rate from $A(\tau)$. The analysis of the data was made with a weighted nonlinear least-squares algorithm on a FACOM M-380Q computer in this institute. For solutions of polymer concentration lower than 19.9×10^{-4} g cm^{-3}, the decay rates Γ, which are equal to the first cumulant, were estimated both by fitting the data to single-exponential decay curves and by using the histogram method of narrow unimodal distributions of the decay rate.[16] The Γ values thus estimated were consistent with each other to within ±2–3%. For solutions of polymer concentration equal to or higher than 44.7×10^{-4} g cm^{-3}, the decay rates at higher angles were successfully estimated by using the histogram method of broader unimodal distributions of the decay rate.

III. Results and Discussion

Profile of Autocorrelation Functions. All $A(\tau)$ curves for six solutions of mass concentration c ranging from 2.08×10^{-4} (S21) to 7.24×10^{-3} g cm^{-3} (S724) were single-exponential-type decays, except for two highest polymer concentration solutions of S447 and S724 at higher scattering angles. Here we retain the previous coding[14a] of these solutions Sff, ff representing the polymer mass concentration expressed in 10^{-5} g cm^{-3} units. The decay rates $\Gamma(q,c)$ were estimated as functions of the scattering vector q and c, their normalized second moment (the variance) resulting in 0.016–0.045 (Table I). The small values of the variance at lower polymer concentration solutions guaranteed that we observed a dynamic process of particles composed of near-monodisperse sizes. It may be worthwhile to note here that $A(\tau)$ for solutions S73 and for solutions of higher c came to give wrong but double-exponential types of decay curves unless the solutions were prepared under careful heat treatment.

Table I
Dynamic Characteristics for a Styrene–Butadiene Diblock Copolymer in n-Decane at 25 °C in the Polymer Concentration Region Denoted as Region III

solution code	c, 10^{-4} g cm^{-3}	$10^8 D$, cm^2 s^{-1}	R_H, nm	k_D, cm^3 g^{-1}	variance, μ_2/Γ^2
S724	72.4	7.33 ± 0.08	34.8 ± 0.4		0.045
S447	44.7	6.82 ± 0.06	37.4 ± 0.3		0.032
S199	19.9	6.31 ± 0.04	40.5 ± 0.2		0.025
S73	7.32	6.03 ± 0.03	42.4 ± 0.2		0.026
S57	5.69	5.97 ± 0.03	42.8 ± 0.2		0.019
S21	2.08	5.90 ± 0.04	43.3 ± 0.3		0.016
$c \to 0$	0.0	5.87 ± 0.04[a]	43.5 ± 0.3[b]	34.8 ± 0.9[a]	

[a] Obtained with the simple extrapolation of $D(c)$ data in the present concentration region to $c \to 0$. See eq 1. [b] Calculated from D_0 by using eq 2.

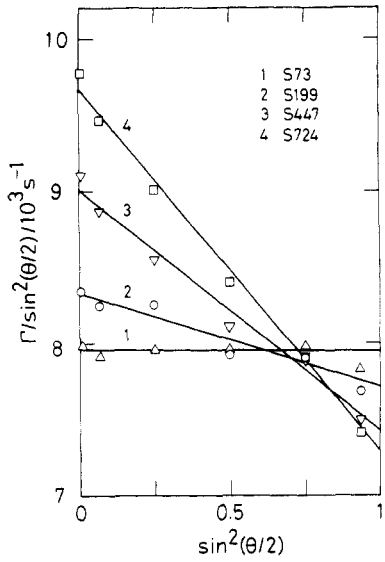

Figure 1. Scattering angle (θ) dependences of the first cumulant Γ measured for a styrene–butadiene diblock copolymer SB1 in n-decane of four different polymer concentrations in dilute solution region. The letters ff of solution code Sff represent the polymer concentration expressed in a 10^{-5} g cm^{-3} unit; e.g., S73 denotes the solution of concentration 7.32×10^{-4} g cm^{-3}.

Extrapolation of Γ to Zero Scattering Vector and to Infinite Dilution. At $q \to 0$, $\Gamma(q=0,c)$ is put equal to $D(c)q^2$ with $D(c)$ the diffusion coefficient at finite polymer concentration c. Figure 1 shows the extrapolations of $\Gamma(q,c)$ to $q = 0$, where $\Gamma(q,c)/q^2$ values at four polymer concentrations of $c = 7.32 \times 10^{-4}$ (S73) to 7.24×10^{-3} g cm^{-3} (S724) are plotted against q^2. The data at each c are well represented by straight lines 1–4 in Figure 1. It is interesting that the slopes are *negative* and the absolute magnitudes of the slopes decrease with decreasing c, reaching zero (i.e., $\Gamma(q,c)/q^2$ becoming constant) at $c \leq 7.32 \times 10^{-4}$ g cm^{-3} (S73). Four lines (1–4) cross each other around $\sin^2(\theta/2) = 0.75$ ($\theta = 120°$) accord-

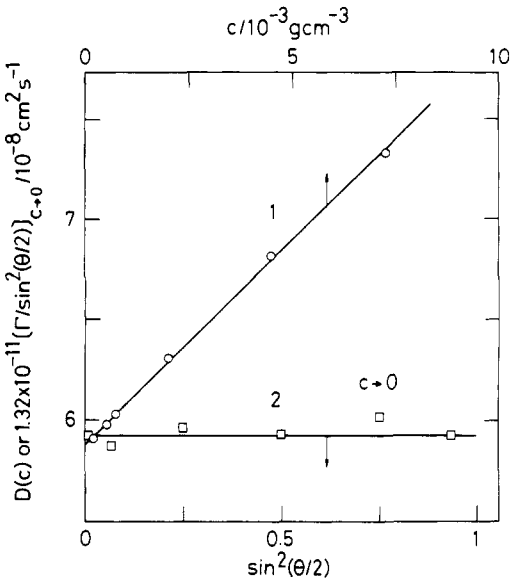

Figure 2. Diffusion coefficients $D(c)$ plotted against the polymer concentration c (line 1) and the first cumulant extrapolated to infinite dilution $(\Gamma/q^2)_{c\to 0}$ plotted against q^2 (line 2) for dilute solutions of SB1 in n-decane at 25 °C. The ordinate for the latter is converted into the unit of the diffusion coefficient ($cm^2\ s^{-1}$).

ingly. Consequently, at each constant q, $\Gamma(c,q)/q^2$ comes to show linear dependence against c, and the coefficient decreases with increasing q, changing sign from positive to negative, though the dependences are not illustrated here. This change of sign in the slopes of the Γ/q^2 vs c plots resembles apparently the case of homopolymers in good solvents.[17] However the negative slopes in Γ/q^2 vs q^2 plots (Figure 1) are in clear contrast to *positive* ones for homopolymers in good[17] and Θ[18] solvents at usual dilute polymer concentrations. Constancy of $\Gamma(q,c)/q^2$ against q^2 such as shown for S73 (line 1 in Figure 1) has already been observed for solutions of lower c (S21, S57), illustrated in region III of Figure 7 in previous work.[14a] The constant behavior is characteristic of translation diffusions and is ascribed to the translational diffusion motion of near-monodipserse micellar particles as a whole. The negative slopes in Γ/q^2 vs q^2 and the decrease in Γ/q^2 with c at larger q (Figure 1) might be related to *internal* motions in the micellar particles. The detail will be discussed in later sections.

Four extrapolated values of Γ/q^2 to $q = 0$, i.e., $D(c)$, obtained in Figure 1 and two $D(c)$ obtained previously in region III[14a] are tabulated in Table I and are plotted against the polymer concentration in Figure 2 with a symbol of unfilled circles. The $D(c)$ values show good linearity with c as is represented by the solid straight line 1 in Figure 2. Assuming that the simple extrapolation of the data to $c = 0$ gives solution characteristics of the SB diblock copolymer in the present concentration region (region III),[14a,19] we could represent the characteristics with the translational diffusion coefficient at infinite dilution D_0 and the concentration coefficient k_D, which are defined by

$$D(c) = D_0(1 + k_D c) \quad \text{(region III)} \qquad (1)$$

The result was that $D_0 = 5.87 \times 10^{-8}\ cm^2\ s^{-1}$ and $k_D = 34.8\ cm^3\ g^{-1}$. The equivalent hydrodynamic radius (Stokes radius) R_H defined by

$$R_H = k_B T/(6\pi\eta_0 D_0) \quad \text{(region III)} \qquad (2)$$

was also evaluated as $R_H = 43.5$ nm. These values are listed in Table I. They represent the translational diffusion of micellar particles which are made of intermolecular association between the SB copolymers, as mentioned above.

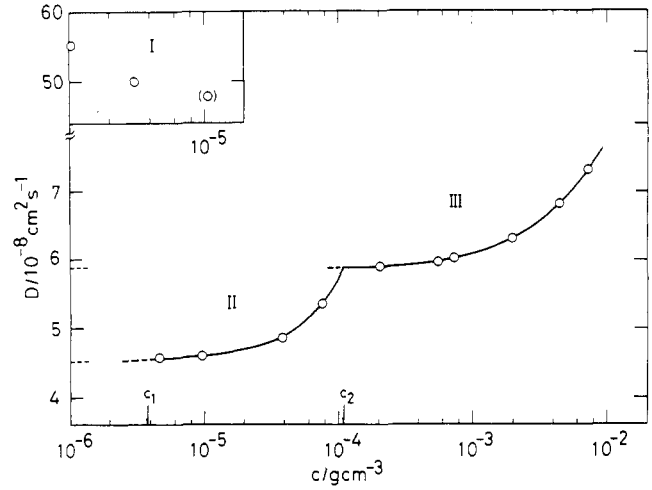

Figure 3. Concentration-dependent double-step transition phenomena of the translational diffusion coefficient $D(c)$ measured for SB1 in n-decane at 25 °C. The solution that yielded the data point in parentheses in region I was prepared in a different way: First, it was prepared according to the procedure described in experiment, then filtered again through a 0.1-μm Millipore filter, and finally heated overnight at 50 °C. The concentrations c_1 and c_2 denote the crossover concentrations, where the $D(c)$ values become discontinuous and the differentiation between the concentration regions I, II, and III is made. The regions I, II, and III are referred to in the text.

The simply linear extrapolations of $\Gamma(q,c)/q^2$ to $c = 0$ at constant q gave $\Gamma(q,c=0)/q^2$ values. The values are plotted against q^2 in Figure 2 with a symbol of squares. They are independent of q^2, as is represented by data-fitted straight line 2, and $\Gamma(0,0)/\sin^2(\theta/2) = 7820\ s^{-1}$. This value gives $D_0 = 5.92 \times 10^{-8}\ cm^2\ s^{-1}$, which agrees with the previous D_0 value, $5.87 \times 10^{-8}\ cm^2\ s^{-1}$, to within 0.8%.

Translational Diffusion Motions and the Transition Behavior of *D*. In order to make clear a connection between the $D(c)$ data in a previous study[14a] and those in the present one, six $D(c)$ values obtained here are plotted against the logarithmic concentration c in Figure 3. The present data, obtained from region III, complete the whole profile of a double-step transition behavior of $D(c)$ for the SB diblock copolymer in n-decane at a concentration ranging widely from 1×10^{-6} to $7.24 \times 10^{-3}\ g\ cm^{-3}$. To our knowledge, it is the first observation of a transition in $D(c)$ as a function c. The transition occurs at the concentrations c_1 and c_2, which are $c_1 \simeq 3.8 \times 10^{-6}$ and $c_2 \simeq 1.1 \times 10^{-4}\ g\ cm^{-3}$, respectively. In these crossover regions, the decay rate distributions $G(\Gamma)$ defined by the inverse Laplace transformation of $A(\tau)$ as[16] $A(\tau) = 1 + \beta[\int_0^\infty G(\Gamma)\exp(-\Gamma\tau)\,d\Gamma]^2$ were found to be still unimodal (narrow), as is typically shown in Figure 4 for a solution S21 in region III, the solution concentration of which is very close to c_2. The narrow unimodal distributions indicate that the particle changes its molecular form drastically around c_1 or c_2.

In region I ($c < c_1$) of Figure 3, the diffusion motion occurs of the single SB molecule which disperses molecularly with the intramolecularly collapsed S subchain (the microphase segregation in the single molecule).[1,9,10] An upturn in $D(c)$ would better conform to the picture of a collapsed S subchain in these extremely dilute conditions. In region II ($c_1 < c < c_2$), the diffusion motion occurs of a huge but loosely packed micelles which is formed due to weak attractive interactions between inter-

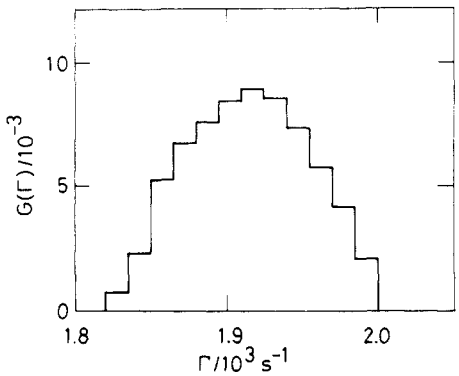

Figure 4. Decay rate distribution $G(\Gamma)$ estimated from $A(\tau)$ for S21 solution at $\theta = 60°$ by using the histogram method. The mean decay rate was 1930 s^{-1}, and the variance was 0.005.

molecular S chains of great numbers.[14a] The numbers cannot be ascertained at present for lack of available data, but brief a discussion will be made in the Appendix. In region III ($c > c_2$), the compactly associated micelles (polymolecular micelles[1]) perform the translational diffusion motion. The micelle is nearly monodisperse, as was guaranteed by the small values of the variance for $A(\tau)$. It has a hydrodynamic radius $R_H = 43.5$ nm (Table I). The molecular weight of the micelle is 9.7×10^6, which was determined by the intrinsic viscosity,[14a] and shows that the micelle is constructed from 100 pieces of the SB copolymers of which the S parts associate intermolecularly and collapse to a hard core, while the B parts swell and cover the core, forming the outer shell.

Anomalous concentration dependence of $D(c)$, which appears here as a double-step transition of D, may embody a sense of the closed association proposed long ago by Elias.[1,7,8] The existence of region I is an observation of especial importance. In other words, micellization starts to occur around $c = c_1$. This concentration is considered to be the cmc for the present SB/n-decane solution system. In this connection, it may be interesting to note here a theoretical work on cmc behavior,[20] though it treats mixtures of AB diblock copolymers in melts of homopolymer A.

Micellar Structure in Region III. As follows, a "two-phase" concentric spheres description is pursued for analysis of the micellar structure; i.e., the micelle is described by two concentric spheres of the total micellar radius R and of core radius r_c with uniform densities d_B and d_c for the shell and the core parts, respectively. According to an approach analogous to that used by Kerker et al.,[21] the particle scattering function $P(q)$ and the apparent radius of gyration $R_{G,app}$ for the micellar particle composed of the S core and the B shell can be expressed as follows:

$$P(q) = [f(qR) + (r_c/R)^3 z f(qr_c)]^2/[1 + (r_c/R)^3 z]^2 \quad (3)$$

$$R_{G,app}^2 = (3/5)R^2[1 + (r_c/R)^5 z]/[1 + (r_c/R)^3 z] \quad (4)$$

$$f(x) = (3/x^3)(\sin x - x \cos x) \quad (5)$$

$$z = (w_S \nu_S / w_B \nu_B) - 1 = -2 + 1/(1 - y) \quad (6)$$

$$y = w_S \nu_S / (w_S \nu_S + w_B \nu_B); \quad w_S + w_B = 1 \quad (7)$$

Here y is the weight-fraction refractive index increment of the core (S) part with w_S (or w_B) and ν_S (or ν_B) the weight fraction and the refractive index increment of the core S (or the shell B) subchains, respectively. If the S core has the same density as that in the bulk state, i.e., $d_c = 1.05 \pm 0.2$ g cm^{-3}, the core radius of N pieces of S subchains r_c can be estimated from the equation[22]

$$r_c = [(NM_{PS}/N_A d_c)/(4\pi/3)]^{1/3} = (7.23 \pm 0.05) \times 10^{-2}(NM_{PS})^{1/3} \text{ nm} \quad (8)$$

where M_{PS} represents the weight-average molecular weight of the S subchain in a single SB diblock copolymer and N_A the Avogadro number. With the experimental values $N = 100$ and $M_{PS} = 2.85 \times 10^4$, we obtained $r_c = 10.2 \pm 0.1$ nm, which is equal to the hydrodynamic radius of the core S part, $R_{H,S}$. Insertion of the values $r_c = 10.2 \pm 0.1$ nm, $R = R_H = 43.5 \pm 0.3$ nm, and $y = 0.3778$ ($w_S = 0.293$; $\nu_S = 0.189$, $\nu_B = 0.129$ at 488 nm at 25 °C)[14a] into eq 4 gave $R_{G,app} = 33.8 \pm 0.2$ nm. For the present system, we obtain the ratio $R_{G,app}/R_H \equiv \rho = 0.78$ accordingly. The value conflicts with the usual one for linear flexible homopolymers $R_G > R_H$ (e.g., $\rho_{exptl} = 1.50$)[17] but agrees with that for rigid spheres $\rho_{theory} = 0.775$.[29] This result is conformable to the "two-phase" concentric sphere description of the present system.

The PB density in the shell, if the density were assumed to be uniform, was evaluated to be $d_B = 3.36 \times 10^{-2}$ g cm^{-3} by using an equation similar to eq 8[4] as follows

$$(4\pi/3)R^3 = (N/N_A)[(M_{PS}/d_c) + (M_{PB}/d_B)] \quad (9)$$

with $M_{PB} = 6.88 \times 10^4$, $d_c = 1.05$ g cm^{-3}, and $N = 100$. The small d_B value indicates that the PB subchains are fully extended in the shell. This situation is assessed as follows. Assume that the shell is approximately composed of N rays of the Gaussian B subchain of mean-square radius of gyration $R_{G,B}^2$. The apparent radius of gyration $R_{G,app}$ has the relation,[22] independent of N

$$R_{G,app}^2 = (3/5)r_c^2 y + (1 - y)R_{GB,int}^2 \quad (10)$$

for $N \to \infty$. $R_{GB,int}^2$ represents the mean-square interchain dimension for B chains in the shell[22]

$$R_{GB,int}^2 = 4\{(3/4) + (r_c/D_B)^2 + (7/3\pi^{1/2})(r_c/D_B)[1 + (9\pi^{1/2}/14)(r_c/D_B)]/[1 + (2/\pi^{1/2})(r_c/D_B)]\}R_{G,B}^2 \quad (11)$$

$$D_B = 2R_{G,B} \quad (12)$$

Optimization of the $R_{G,B}$ value in eqs 10–12 with the values $R_{G,app} = 33.8 \pm 0.2$ nm, $r_c = 10.2 \pm 0.1$ nm, and $y = 0.3778$ gave the consistent $R_{G,B}$ value $D_B = 2R_{G,B} = 39.4 \pm 0.6$ nm. Since the unperturbed value of a single homopolymer B chain $R_{GB,homo}$ is 8.8–11.0 nm,[23] the expansion factor α_S defined by $\alpha_S = R_{G,B}/R_{GB,homo}$ becomes 2.3–1.8. The extremely large value of α_S obtained for such a low molecular weight chain as $M_{PB} = 6.88 \times 10^4$ indicates that the B subchains are in a highly extended state in the shell. In this stage, however, it should be mentioned that the shell might be neither of concentric spherical shape nor of uniform density since the shell was found to fluctuate in the concentration of B chains, as is revealed in later sections.

It is interesting to compare the micellar structure revealed above with the result obtained by Plestil and Baldrian.[4] They observed by small-angle X-ray scattering (SAXS) a micellar formation for the similar polymer/solvent system to but at slightly higher concentration than ours: a SB diblock copolymer ($M_n = 6.47 \times 10^4$, 24 wt % PS) in n-heptane at the polymer concentration ranging from 5.4×10^{-3} to 38.3×10^{-3} g cm^{-3}. The obtained structure parameters of the micelles are $N = 175$, $r_c = 10.6$ nm, $R_{G,app} = 19.9$ nm, and $R = 27.6$ nm. Similar $R_{G,app}$ values of 17.1–19.5 nm were also reported by Bluhm and Whitmore[24] with SAXS for SB diblock copolymers of $M = 7.7 \times 10^4$–10.55×10^4 (28.6–11.8 wt % PS) in

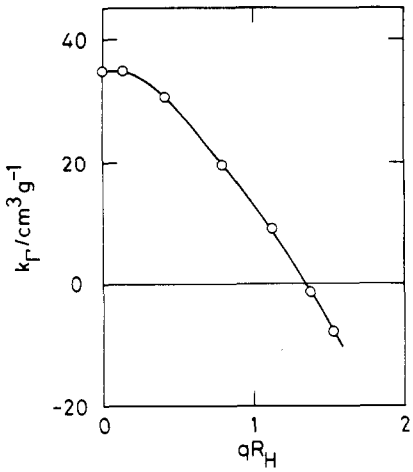

Figure 5. Concentration coefficient of the first cumulant k_Γ plotted as a function of qR_H for SB1 in *n*-decane at 25 °C.

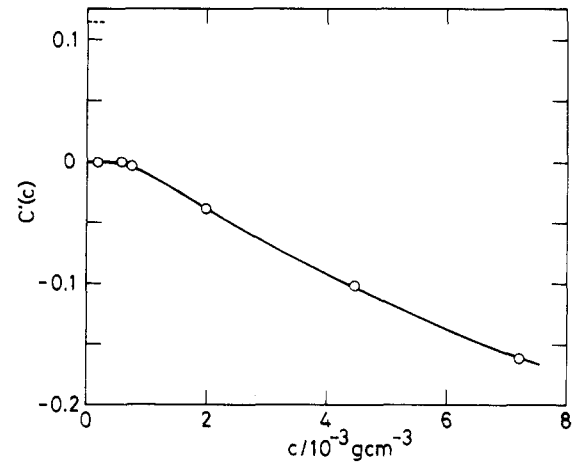

Figure 6. Concentration dependence of the coefficient $C'(c)$ appearing in the expansion of Γ/q^2 up to powers of q^2 (eq 16) for SB1 in *n*-decane at 25 °C. A relation $C'(0) = C(R_G/R_H)^2$ holds between the usual coefficient C and the present one $C'(0)$ at $c = 0$. A horizontal broken line at $C'(0) = 0.114$ represents the value for regular star molecules of infinite numbers of rays.

n-heptane at the concentration 2×10^{-3}–1×10^{-2} g cm^{-3}.

In addition, it is worthwhile to refer to the theoretical predictions on N and r_c. Let p_S and p_B be the degrees of polymerization of S and B subchains in the SB copolymer, respectively. Based on a two-phase concentric spheres representation for micelles well past the cmc, i.e., for micelles composed of large numbers of N, the micellar structures are classified into two types:[25] one is the case $p_S \gg p_B$, where the insoluble core is much larger than the soluble B part, and the other is the reverse, $p_S \ll p_B$. It may be reasonable for the former to assume a uniform polymer density profile in both the core and the shell parts of the micelle,[26] but in the latter case the density in the shell may decrease with increasing the distance from the micellar center.[25] Both cases give the following scaling laws:[24-26]

for $p_S \ll p_B$ (ref 25)

$$N \simeq p_S^{4/5};\quad r_c \simeq p_S^{3/5}a;\quad R \simeq p_S^{4/25}p_B^{3/5}a \qquad (13\text{-}1)$$

for $p_S \gg p_B$

$$N \simeq p_S;^{25,26}\quad r_c \simeq R \simeq p_S^{2/3}a;^{25,26}\quad r_B \simeq p_B^{1/2}\ ^{24} \qquad (13\text{-}2)$$

Here r_B denotes the shell thickness and a a typical monomer size. The prefactors in eq 13 are ignored[25] or expressed by various parameters.[26] Quantitative prediction from these theoretical equations can be obtained only through a numerical computation made under some assumptions on the involved several parameters, which parameters concern polymer–polymer or polymer–solvent interactions and interfacial tension.[26] However, elimination of p_S in eqs 13-1 and 13-2 gives the molecular weight independent a value as $a = r_cN^{-3/4}$ and $a = r_cN^{-2/3} = RN^{-2/3}$, respectively. For the present system, the former relation predicted that $a = 0.32$ nm. This value is consistent with $a = 0.24$ nm which was calculated from the third relation of eq 13-1, $a \simeq RN^{-1/5}p_B^{-3/5}$, with $N = 100$, $R_H = 43.5$ nm, and $p_B = M_{PB}/54.1 = 1270$ ($r_c = 10.2$ nm and $p_S = M_{PS}/104.1 = 274$).

***c* and *q* Dependences of $\Gamma(q,c)$.** On the analogy of the concentration dependence of $\Gamma(q,c)$ for linear flexible chains in solution,[27] we can use the following expression for the present diblock copolymer/*n*-decane solution system:

$$\Gamma(q,c)/q^2 = [\Gamma(q,0)/q^2][1 + k_\Gamma(q)c] \qquad (14)$$

At $q \to 0$, eq 14 reduces to eq 1 with D_0 and k_D defined by

$$D_0 \equiv [\Gamma(0,0)/q^2];\quad k_D \equiv k_\Gamma(q=0) \qquad (15)$$

The concentration coefficient k_Γ may depend on interactions between the component (especially B subchains) segments belonging to different micelles and may also depend on the component excluded volume, the structure factors, and the mobility of micelles. The k_Γ values at given q for the present solution system were evaluated from the data shown in Figure 1 and are plotted against qR_H in Figure 5. k_Γ is constant at $qR_H < 0.15$ but decreases sharply at $qR_H > 0.15$ with increasing qR_H, going down to negative values at larger qR_H. Positive k_Γ at $qR_H < 1.3$ is attributed mainly to the positive k_D (=34.8 cm^3 g^{-1}) of the translational diffusion motion of the SB copolymer micelles as a whole. Decrease of k_Γ with increasing qR_H and negative k_Γ at $qR_H > 1.3$ may be related to the appearance of new modes characteristic of copolymer chain nature. The former (the decrease of k_Γ at $k_\Gamma > 0$) might signal the combined influence of normal modes of B subchains and the diblock copolymer mode. Here the diblock copolymer mode means the relative center-of-mass motion of B subchains (the shell) with respect to the S core in the single micellar particle, particularly the concentration fluctuation in the shell. However, the latter (negative k_Γ) might be due predominantly to the diblock copolymer mode. This mode might induce attractive (negative) interactions between B subchains in different micelles. Recently, Benmouna et al.[28] have predicted in their theoretical works on diblock copolymer solutions that the mode due to the internal concentration fluctuations will show negative k_Γ, while positive k_Γ is predicted to the mode of the translational diffusion of the molecule as a whole.

On the Γ vs q dependence, the following general expansion of $\Gamma(q,c)$ in a power series of q^2 is obtained[29] for linear chains and for branched structure polymers in dilute solution:

$$\Gamma(q,c)/q^2 = D(c)[1 + CR_G^2(c)q^2 ...]$$
$$= D(c)[1 + C'(c)R_H^2(c)q^2 ...] \qquad (16)$$
$$C'(c) = C[R_G(c)/R_H(c)]^2 \qquad (17)$$

For $c \to 0$, eqs 16 and 17 become

$$[\Gamma(q,c)/q^2]_{c=0} = D_0[1 + C'(0)R_H(c=0)q^2 ...] \qquad (18)$$

$$C'(0) = C\rho^2;\quad \rho \equiv R_G(c=0)/R_H(c=0);\quad R_G^2(c=0) \equiv R_{G,app}^2 \qquad (19)$$

where C or $C'(0)$ is a characteristic constant that depends on the molecular architecture. We tried to use this expression for the present copolymer/solvent system and to evaluate the q^2 coefficient $C'(c)$ from Figure 1 with $R_H(c)$ at finite polymer concentration c. Figure 6 shows this result, where $C'(c)$ is plotted against c. The $C'(c)$ value is constant (zero) in dilute regions of $c \simeq 2 \times 10^{-4}$–$7.5 \times 10^{-4}$ g cm^{-3} and then decreases (negative) with increasing c. The value $C' = 0$ at $c \simeq 0$, i.e., $C = 0$, is equal to that for rigid spheres[35] and is in contrast to the usual positive values for molecules of flexible linear or branched structures of various kinds, as is typically given by a value $C'(0) = 0.114$ for regular star molecules of infinite numbers of rays ($N \rightarrow \infty$).[29] The negative $C'(0)$ at $c > 7.5 \times 10^{-4}$ g cm^{-3} might be attributed to intermiceller interactions which are characteristic of the micellar structure mentioned already.

Appendix

Micellar Structure in Region II. Here, the particle structure formed in region II is discussed briefly, though it is still unclear as described below. Let us first consider an all or none process in region II; that is, the single copolymer of region I (molecular weight M_I) is in equilibrium with the micelles of region III (N pieces of copolymers with molecular weight M_N). The mixture of species with molecular weights M_I and M_N, with weight fractions w_I and $1 - w_I$, respectively, gives, by definition, the weight-average molecular weight M_w and the diffusion coefficient D, which should be expressed by the z-average diffusion coefficient D_z as follows:

$$M_w = w_I M_I + (1 - w_I) M_N \quad \text{(A1)}$$

$$D \equiv D_z = [w_I M_I D_I + (1 - w_I) M_N D_N]/M_w \quad \text{(A2)}$$

with D_I and D_N the diffusion coefficients of the single and micellar particles, respectively. It follows from elimination of M_w from eqs A1 and A2 that

$$D_z = \{D_N + [w_I M_I/(1 - w_I) M_N] D_I\}/ [1 + w_I M_I/(1 - w_I) M_N] \quad \text{(A3)}$$

With experimental values $M_N/M_I = 100$, $D_N = D_0$(region III) $= 5.87 \times 10^{-8}$ cm^2 s^{-1}, and $D_I = D_0$(region I) $= 54.3 \times 10^{-8}$ cm^2 s^{-1}, it is expected that $D_I \geq D_z \geq D_N$, which conflicts with experimental D in region II, where D(region II) $< D_N$. The solutions in region II are thus never composed of mixtures of the particles formed in regions I and III.

Let us secondly consider that the particles in region II are cylindrical rods of length L and radius r. For this shape of particles, the following expressions are available for D_0,[30] the second virial coefficient A_2,[31] and the concentration-dependent factor of the friction coefficient k_f:[32,33]

$$D_0 = k_B T \ln (L/r)/(3\pi\eta_0 L)$$

$$R_H = L/2 \ln (L/r) \quad \text{(A4)}$$

$$A_2 = (\pi N_A/2)(r/M_L^2) \quad \text{(A5)}$$

$$k_D = 2A_2 M_w - k_f - v \quad \text{(A6)}$$

$$k_f = (k_B T/3\eta_0)(3A_2 N_A^{1/2}/2\pi)^{2/3}(M_w^{1/3}/D_0) \quad \text{(A7)}$$

where M_L is the molar mass per unit length defined by $M_L = M_w/L$ and v is the partial specific volume of the particle. k_D can be given from eqs A4–A7 as a function of r, L, and/or M_L alone

$$k_D + v = \pi N_A (rL/M_L)\{1 - [(3/4)^2(L/r)]^{1/3}/\ln (L/r)\} \quad \text{(A8)}$$

Experimental values of D_0 (or R_H, $D_0 = 4.49 \times 10^{-8}$ cm^2 s^{-1})[14a] were obtainable with reasonable r and L values. However, the experimental positive k_D (=2450 cm^3 g^{-1})[14a] could never be obtained because eq A8 always gave negative k_D values for any reasonable r, L, and/or M_L value.

References and Notes

(1) Tuzar, Z.; Kratochvil, P. *Adv. Colloid Interface Sci.* **1976**, *6*, 201 and references cited therein.
(2) Kotaka, T.; Tanaka, T.; Hattori, M.; Inagaki, H. *Macromolecules* **1978**, *11*, 138. Kotaka, T.; Tanaka, T.; Inagaki, H. *Polym. J.* **1972**, *3*, 327.
(3) Utiyama, H.; Takenaka, K.; Mizumori, M.; Fukuda, M.; Tsunashima, Y.; Kurata, M. *Macromolecules* **1974**, *7*, 515.
(4) Plestil, J.; Baldrian, J. *Makromol. Chem.* **1975**, *176*, 1009.
(5) Price, C.; McAdam, J. D. G.; Lally, T. P.; Wood, D. *Polymer* **1974**, *15*, 228.
(6) Mandema, W.; Zeldenrust, M.; Emeis, C. A. *Makromol. Chem.* **1979**, *180*, 1521. Mandema, W.; Emeis, C. A.; Zeldenrust, M. *Macromolecules* **1979**, *180*, 2163.
(7) Elias, H.-G. *J. Macromol. Sci., Chem.* **1973**, *7*, 601.
(8) Elias, H.-G. In *Light Scattering from Polymer Solutions*; Huglin, M., Ed., Academic Press: London, 1972; Chapter 9.
(9) Sadron, C. *Pure Appl. Chem.* **1962**, *4*, 347.
(10) Pourchly, J.; Zivny, A.; Sikora, A. *J. Polym. Sci., Polym. Phys. Ed.* **1972**, *10*, 151; *J. Polym. Sci., Part C: Polym. Symp.* **1972**, *39*, 133.
(11) Plestil, J.; Baldrian, J. *Makromol. Chem.* **1973**, *174*, 183.
(12) Tuzar, Z.; Kratochvil, P. *Makromol. Chem.* **1972**, *160*, 301.
(13) Tuzar, Z.; Petrus, V.; Kratochvil, P. *Makromol. Chem.* **1974**, *175*, 3181.
(14) (a) Tsunashima, Y.; Hirata, M.; Kawamata, Y. *Macromolecules* **1990**, *23*, 1089. (b) Nemoto, N.; Tsunashima, Y.; Kurata, M. *Polym. J.* **1981**, *13*, 827.
(15) The crossover polymer concentration c^* may be estimated from the relation $c^* \simeq [\eta]^{-1}$ with $[\eta] = 53.5$ cm^3 g^{-1} for the present SB diblock copolymer in *n*-decane at 25 °C.[14a] The estimated c^* value, $c^* = 1.87 \times 10^{-2}$ g cm^{-3}, is still larger than the concentration region studied in this paper.
(16) Gulari, E.; Gulari, E.; Tsunashima, Y.; Chu, B. *J. Chem. Phys.* **1979**, *70*, 3965. Tsunashima, Y.; Nemoto, N.; Kurata, M. *Macromolecules* **1983**, *16*, 584.
(17) For example: Tsunashima, Y.; Hirata, M.; Nemoto, N.; Kurata, M. *Macromolecules* **1987**, *20*, 1992. Nemoto, N.; Makita, Y.; Tsunashima, Y.; Kurata, M. *Macromolecules* **1984**, *17*, 425.
(18) For example: Tsunashima, Y.; Hirata, M.; Nemoto, N.; Kajiwara, K.; Kurata, M. *Macromolecules* **1987**, *20*, 2862. Tsunashima, Y.; Nemoto, N.; Kurata, M. *Macromolecules* **1983**, *16*, 1184.
(19) At $c < 1.1 \times 10^{-4}$ g cm^{-3}, we have already observed another two types of concentration dependence of $D(c)$,[14a] as described in the Introduction. The dependences are distinguished from the present one and are regarded as the behavior characteristic of the two concentration regions: region I ($c < 3.8 \times 10^{-6}$ g cm^{-3}) and region II (3.8×10^{-6} g cm$^{-3} < c < 1.1 \times 10^{-4}$ g cm^{-3}), respectively.
(20) Leibler, L.; Orland, H.; Wheeler, J. C. *J. Chem. Phys.* **1983**, *79*, 3550.
(21) Kerker, M.; Kratohvil, J. P.; Matijevic, E. *J. Opt. Sci. Am.* **1962**, *52*, 551. Plestil, J.; Baldrian, J. *Makromol. Chem.* **1973**, *174*, 183.
(22) Tsunashima, Y.; Hirata, M.; Kurata, M. *Bull. Inst. Chem. Res., Kyoto Univ.* **1988**, *66*, 33. The equation presented in ref 11 contains a misprint: the coefficient 0.145 should read 0.0723.
(23) Kurata, M.; Tsunashima, Y. In *Polymer Handbook*, 3rd. ed.; Brandrup, J., Immergut, E. H., Eds.; Wiley: New York, 1989; Chapter VII-1.
(24) Bluhm, T. L.; Whitmore, M. D. *Can. J. Chem.* **1985**, *63*, 249.
(25) Halperin, A. *Macromolecules* **1987**, *20*, 2943.
(26) Noolandi, J.; Hong, K. M. *Macromolecules* **1983**, *16*, 1443.
(27) Hammouda, B.; Akcasu, A. Z. *Macromolecules* **1983**, *16*, 1852.
(28) Benmouna, M.; Benoit, H.; Borsali, R.; Duval, M. *Macromolecules* **1987**, *20*, 2620.
(29) Burchard, W.; Schmidt, M.; Stockmayer, W. H. *Macromolecules* **1980**, *13*, 580, 1265. Burchard, W. *Adv. Polym. Sci.* **1983**, *43*, 1.
(30) Perrin, F. *J. Phys. Radium* **1934**, *5*, 497; **1936**, *7*, 1.
(31) Yamakawa, H. *Modern Theory of Polymer Solutions*; Harper & Row: New York, 1971.

(32) Peterson, J. M. J. Chem. Phys. 1964, 40, 2680.
(33) Kubota, K.; Tominaga, Y.; Fujime, S. Macromolecules 1986, 19, 1604.
(34) Thurmond, C. D. J. Polym. Sci. 1952, 8, 607.
(35) Burchard, W.; Eisele, M. Pure Appl. Chem. 1984, 56, 1379.

Registry No. SB (block copolymer), 106107-54-4; *n*-decane, 124-18-5.

Application of the "Spectroscopic Ruler" to Studies of the Dimensions of Flexible Macromolecules. 3. Equation Describing the Relative Diffusion between Polymer Chain Ends

Guojun Liu and J. E. Guillet*

Department of Chemistry, University of Toronto, Toronto, Ontario, Canada M5S 1A1

Received July 24, 1989; Revised Manuscript Received November 14, 1989

ABSTRACT: An equation is derived from probability theories for the relative diffusion between ends of a Gaussian chain. Numerical solution of the derived equation gives the time-dependent end-to-end distance distribution function. As time approaches infinity, the time-dependent end-to-end distance distribution function approaches the Gaussian form regardless of the initial end-to-end distance of the Gaussian chain.

I. Introduction

The end-to-end distance of a polymer chain varies with time due to continuous changes in chain conformations. Variation of the relative separation distance between the end groups originally (at $t = 0$), R, with time is of both theoretical and experimental importance. In a previous paper in this series,[1] the root-mean-square end-to-end distances of end-labeled poly(methyl methacrylate) (PMMA) chains measured using the "Spectroscopic Ruler" technique in nonviscous solvents were found to be consistantly shorter than those determined from intrinsic viscosity measurements. It was suggested that the variations of the relative separation distances between the end groups during the fluorescence lifetime of the donor were partially responsible for the discrepancies.

Further, consider a chemical reaction between two ends of a polymer chain. If the variation in end-to-end distance is due to the relative diffusion between the chain ends and the reaction is diffusion-controlled, approach of the two end groups within an effective reaction radius, R_e, will result in instantaneous reaction. If the distribution function of the end-to-end distance, r, of such a chain is $S(r, R, t)$ at time t, the probability of reaction after time t for the end groups originally separated by $R > R_e$ at time t is

$$\rho(t,R) = \int_0^{R_e} S(r, R, t)\, dr \qquad (1)$$

Assuming that there are N molecules in the system and the end-to-end distance distribution function at time $t = 0$ is given by $P(R)$, the rate of reaction at time t is

$$\frac{dN(t)}{dt} = N \int_{R_e}^{m_z} P(R) \int_0^{R_e} \left(\frac{dS(r, R, t)}{dt}\right) dt \qquad (2)$$

Under Θ conditions, the equilibrium end-to-end distance distribution function of polymer chains can be described by the well-known Gaussian form.[2] The Gaussian probability function can then be related to a potential energy, as has been shown by Katchalski-Katzir et al.[3] The relative diffusion between the ends can now be described as the diffusion of particles in a potential field and is soluble by the Smoluchowski equation.[4]

In this paper, an approach to the derivation of the diffusion equation using pure probability theory is presented and compared to the approach using the Smoluchowski equation. The diffusion equation is solved numerically for chains starting with either $R < R_m$, $R = R_m$, or $R > R_m$, where R_m is the most probable end-to-end distance of the Gaussian chain at various times t. The statistical parameters for the chain are chosen on the basis of those PMMA samples described previously.[1]

II. Theory

The relative diffusion between chain ends can be pictured as many small jumps of distance δ occurring at very high frequency ψ. We are interested only in changes in the relative distances of chain ends. The coordinate system can be chosen in such a fashion that one end group is kept unchanged with time in the origin. The change in end-to-end distance, r, is depicted as solely caused by movement of the other end in space.

If spherical coordinates are used, the moving end can be pictured as making jumps from one sphere to another. The concentric spheres all have their centers at the origin. At time $t = 0$, the moving end is located at (R, θ_0, ϕ_0) and the end-to-end distance is R. At time t, the acceptor end group moves to position (r, θ, ϕ) and the end-to-end distance is then r. By making the next jump at time $(t + 1)/\psi$, the moving end group can be on any sphere with a radius ranging from $r - \delta$ to $r + \delta$, as shown in Figure 1. The probability for the moving end to be located on different spheres at time $(t + 1)/\psi$ is not the same for two reasons.

(1) The linkage between the polymer ends makes completely random jumps improbable. Let us discuss the probability of making two jumps. One jump decreases the end-to-end distance by δ, and the other increases it by δ. At time $(t + 1)/\psi$, if the donor makes the first jump, the end-to-end distance will be $r - \delta$; otherwise, it will be $r + \delta$. The probability $\rho(r \rightarrow r - \delta)$ for the occurrence of an end-to-end distance of $r - \delta$ for a chain of n

0024-9297/90/2223-2969$02.50/0